sustainability

MDPI

Article

Battery Thermal Management: An Application to Petrol Hybrid Electric Vehicles

Raja Mazuir Raja Ahsan Shah [1,*], Mansour Al Qubeissi [2], Hazem Youssef [2] and Hakan Serhad Soyhan [3,4]

[1] College of Engineering Technology, University of Doha for Science and Technology, Doha 24449, Qatar
[2] School of Mechanical Engineering, Coventry University, Coventry CV1 2JH, UK
[3] Department of Mechanical Engineering, Esentepe Campus, Sakarya University, Sakarya 54050, Turkey
[4] Team-SAN Ltd. Sti., Teknokent, Serdivan 54050, Turkey
* Correspondence: mazuirra@yahoo.co.uk

Abstract: Battery thermal management systems (BTMS) in hybrid electric vehicles can be complex and heavy. They tend to increase energy consumption, leading to higher carbon dioxide emissions. In this study, a new approach was investigated for the potential use of four fuel components as coolants for direct liquid-cooled (LC)-BTMS, N-Pentane, N-Hexane, N-Butane, and Cyclo-Pentane. The performance of the fuel components was numerically analysed and CFD modelled using ANSYS Fluent software. Several meshing iterations of the lithium-ion battery (LIB) module were performed to conduct mesh independence check for higher accuracy and less computational time. The LIB module was simulated, in comparison to a free air convection (FAC)-BTMS as a benchmark, at three discharge rates (1C, 1.5C, 2C) for each of the inlet velocity values (0.1, 0.5, 1 m/s). Results show that FAC-BTMS exceeded the LIB module optimal operating temperature range (293–313 K) at 2C. On average, at the worst condition (lowest inlet velocity and highest discharge rate), all fuel components of the LC-BTMS were able to maintain the LIB module temperature below 288 K. That is at least 4.7% cooler compared to FAC-BTMS, which renders the new approach viable alternative to the conventional BTMS.

Keywords: lithium-ion battery; battery cooling; fuel; HEV; energy management

Citation: Raja Ahsan Shah, R.M.; Al Qubeissi, M.; Youssef, H.; Soyhan, H.S. Battery Thermal Management: An Application to Petrol Hybrid Electric Vehicles. *Sustainability* **2023**, *15*, 5868. https://doi.org/10.3390/su15075868

Academic Editor: J. C. Hernandez

Received: 22 January 2023
Revised: 27 February 2023
Accepted: 8 March 2023
Published: 28 March 2023

1. Introduction

Over the past few centuries, the world has relied on fossil fuels as the main energy source to power vehicles with internal combustion (IC) engines. This has come at a great cost to the environment and human health, as 20% of all carbon dioxide (CO_2) emissions originate from road traffic [1]. As a result, electric vehicles (EVs) have begun to dominate the automotive industry to reduce CO_2 gas emissions. In 2015, 550,000 units of EVs were sold, and this subsequently increased to 774,000 units in 2016 [2]. However, EVs have several inherited issues, such as range anxiety [3], long charging time [4], and the availability of charging infrastructures [5]. One of the solutions for these issues is to have different powertrain topologies, such as hybrid electric vehicles (HEVs) [6].

Rechargeable lithium-ion batteries (LIBs) are the most common type of energy storage for HEVs. However, LIBs generate heat while charging or discharging, and if this heat is not dissipated, it affects the battery's performance and causes it to have a reduced lifespan, leading to thermal runaway [7]; thus, the heat generated by LIBs must be adequately thermally managed. For instance, Sato [8] investigated the effect of LIBs operating above 323 K, which showed a decrease in charging efficiency and LIB longevity.

To mitigate these concerns, a battery thermal management system (BTMS) is introduced to cool LIBs at an optimal operating temperature range of 293–313 K [9]. The temperature difference within LIBs could also influence their longevity and be kept below 5 K [10]. Several cooling techniques could be implemented, such as direct and indirect

cooling, and with several cooling media, such as air, liquid, phase-change material (PCM), and heat pipes (HPs) [11].

The heat generation inside LIBs is a complex process that requires knowledge of how the electrochemical reaction rate varies with time, temperature, and current flows. Kim et al. [12] presented the heat generation of LIBs as $\dot{Q} = I\,(U - V) - I\,(T\frac{dU}{dT})$, where $\dot{Q}$, I, U, and V are the rate of heat generation, the electric current passing the cell, open circuit voltage, and the cell voltage of the LIB, respectively. The resistance loss and reversible entropic heat in the electrochemical reaction are denoted by $I\,(U - V)$ and $(T\frac{dU}{dT})$, respectively. During charging and discharging processes, LIBs generate three types of heat: (1) the activation of irreversible heat due to the polarisation of the electrochemical reaction, [13] (2) joule heating due to ohmic losses [14], and (3) reversible reaction due to the entropy change [15].

The LIB thermal runaway is a common issue when it reaches the maximal threshold temperature. The thermal runaway is caused by the exothermic reactions among the anode, cathode, and electrolyte [16]. These exothermic reactions are caused by short circuits, high-speed charging/discharging, and overcharging LIBs [17]. The thermal runaway of a single LIB may lead to the thermal runaway of the entire LIB pack, which causes severe damage [18].

BTMSs can be categorised into three strategies: (1) active, (2) passive, and (3) hybrid [19,20]. Active BTMSs often use air or a liquid cooling medium where the cooling medium can be in either direct or indirect contact with LIBs. Pumps and fans are used to circulate the cooling medium and transfer the heat to the ambient condition. Passive BTMSs implement PCM and HP on the surface of LIBs to improve the heat transfer with the boundaries [11]. Lastly, hybrid BTMSs adapt PCM + air, PCM + liquid, or PCM + HP.

Air-cooled is a preferable BTMS solution due to less weight and system complexity compared to those of liquid-cooled solutions. An efficient air-cooled (AC)-BTMS can remove excess heat generated from LIBs during charging/discharging and maintain the optimal operating temperature. However, in forced AC-BTMSs, air cooling capacity is limited due to poor thermal conductivity, which increases the working temperature and causes thermal imbalances within LIBs under harsh operating conditions, in addition to having difficulty in achieving uniform air distribution [21]. Moreover, forced AC-BTMSs require higher volumetric flow to achieve similar cooling performance to that of other types of BTMS; thus, AC-BTMSs are not efficient in controlling the temperature in LIBs that have fast charging/discharging rates.

For fast charging/discharging applications, direct liquid-cooled (LC)-BTMSs are preferred since they have a higher heat coefficient than AC-BTMSs [22]. A dielectric cooling medium is used in direct LC-BTMSs due to its electrically nonconductive properties and high thermal stability. Direct LC-BTMSs require two to three times less energy compared to AC-BTMSs to maintain the same average temperature of LIBs [23]. One of the dielectric cooling media is oil. The rate of the heat transfer of oil was significantly higher than that of air at the same mass flow rate [24]. However, a newer experiment found that using mineral oil as a dielectric coolant introduced weight to a vehicle, which worsened its performance and increased its energy consumption [25]. The 3M Novec-7000 is another type of dielectric coolant, and it is commonly used in direct LC-BTMSs. For instance, Thakur et al. [22] developed the boiling LIB cooling method using 3M Novec-7000. At a discharge/charge rate (C) of 10C, the performance of direct LC-BTMSs was examined by comparing an AC-BTMS and a boiling LC-BTMS. Using the air-cooled system, the LIB temperature increased to 353–363 K, whereas with total immersion in the 3M Novec-7000, the LIB temperature remained at 308 K.

Implementing indirect LC-BTMSs can be considerably more complicated and expensive than direct LC-BTMSs. Indirect LC-BTMSs are where the cooling media do not get in direct contact with LIBs, and are mainly used to prevent electrical conduction with LIBs whilst dissipating heat. However, there are two issues with indirect LC-BTMSs: (1) leakage

at cooling connections that cause LIBs to short circuit, and (2) high thermal resistance due to the electrically insulating coating that reduces the heat transfer performance [26].

For passive PCM-BTMSs, PCM is designed to surround LIBs. When LIBs heat up, the PCM softens and absorbs the heat. When LIBs cool off, PCM hardens and releases all the heat into the atmosphere. PCM stores thermal energy via the latent heat phase of transitions [27]. Moreover, it has a large amount of latent heat; and during LIBs discharge, it acts as a heat sink. PCM can effectively lower LIBs' maximum temperature and reduce the temperature differences at the end of the discharge cycle [28]. However, there are three disadvantages of PCM-BTMSs, namely (1) low thermal conductivity, (2) leakage problems, and (3) limited capacity of heat absorption after melting [29].

On the other hand, passive HP-BTMSs have high thermal conductivity and are used to maintain the temperature of LIBs within the optimal working temperature range [30]. For example, Nasir et al. [31] implemented HP-BTMS to cool HEVs LIBs, and it was found that the system was able to reduce the maximum LIB temperature by 287.7 K and maintain an average temperature below 323 K [31]. The advantage of using HP-BTMSs is providing a lightweight system with an extended lifecycle. However, the main concern with HP-BTMSs is the relatively high cost compared to other cooling techniques [29].

To reduce the overall weight of HEVs and, subsequently, the vehicle energy consumption, the ideal volume and weight of BTMSs should be less than 40% of the LIB module [32]. These requirements motivate the need to find alternative solutions where fuel (already stored in the tank) has the potential to maintain the LIB's temperature. The concept of using fuel as the cooling medium for BTMSs, introduced in [33], can reduce the weight of EVs and improve vehicle performance and energy consumption.

Many hydrocarbon molecules in petroleum are found as good dielectrics. However, dielectric permittivity can be altered by the number of carbon atoms in the fuel composition. For instance, using N-Heptane as a coolant for BTMSs managed to control the LIB's maximum temperature at discharge rates 1C and 2C by not more than 280.9 K and 290.9 K, respectively, compared to a LIB without BTMS [33]. Fuel must have good material compatibility with LIBs to protect the elastomer seals, copper, and insulation materials from any harm. High flash point reduces the fire risk in high temperatures and improves safety. Fuel components that have dielectric constants (κ) lower than 2 are suitable for direct LC-BTMSs [34].

From the above literature, the challenges are to identify a suitable cooling medium for LIBs that can maintain the optimal operating temperature range and the low-temperature differences between LIBs. Additionally, this approach can reduce the overall weight of HEVs and minimise system complexity. In this paper, we investigated the cooling strategy of petrol components for direct LC-BTMSs using computational fluid dynamics (CFD) for HEVs application. The approach is the first of its kind and has not been revealed elsewhere before, to the best of our knowledge. A commercial software, ANSYS-Fluent, is used to simulate LIB thermal behaviour at different discharge rates. Dielectric components of petrol molecules are investigated for their suitability in BTMSs.

2. Modelling and Parameterisation Study

A transient 3D modelling of LIBs and their enclosure is conducted using the commercial CFD software ANSYS-Fluent. The system design is produced using CATIA V5. Both thermal and electrochemical interactions are accounted for and coupled in the simulation. The main result indicators are the individual LIB maximum temperature, and the temperature differences across the domain and between LIBs. Five cooling media are considered in this study: air, N-Pentane, N-Hexane, N-Butane, and Cyclo-Pentane, based on a direct LC-BTMS strategy. The dimensions and materials used in LIB sub-components are provided in the following sections. In addition, the governing equations used in the numerical simulations are highlighted, along with the coolant properties.

2.1. LIB Module

The LIB module used in this study consists of four LIBs, as shown in Figure 1. The configuration of the LIB module is based on 4S1P (four LIBs in series and one LIB in parallel). Each of the LIBs is connected to two aluminium tabs (positive and negative connections). These tabs are connected via copper busbars to form the LIB module. In total, the sub-components of the LIB module are four LIBs, eight tabs, and three busbars. LIBs are spaced by 5 mm gaps for the cooling medium. The properties of the LIB and tab and busbar are shown in Tables 1 and 2, respectively.

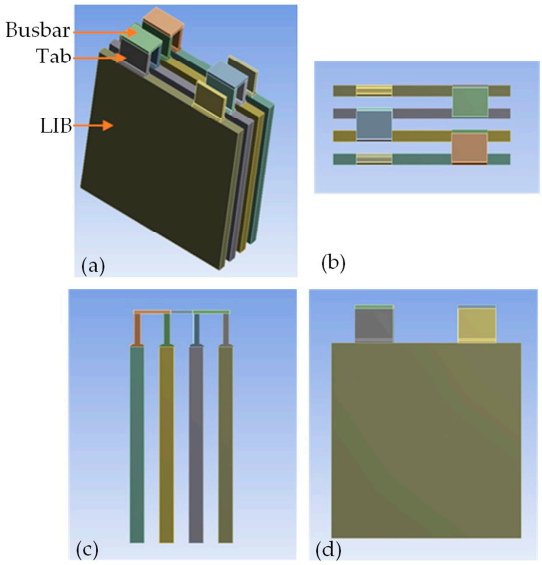

Figure 1. LIB module 4S1P design with busbar and tab with third angle projection view (**a**) isometric view, (**b**) plan view, (**c**) side view, and (**d**) front view.

Table 1. LIB specifications.

Parameters	Value
Nominal capacity (A·h)	14
Max discharge rate (C)	2
Min discharge rate (C)	1
Max module voltage (V)	12
Min module voltage (V)	8.1
Height (mm)	100
Width (mm)	100
Thickness (mm)	5
Density kg·m^3	2092
Specific heat (J/kg·K)	678
Thermal conductivity (W/m·K)	18.2

Table 2. Tab and busbar properties.

Properties	Tab	Busbar
Material	Aluminum	Copper
Density (kg/m^3)	2719	8978
Specific heat (J/kg·K)	871	381
Thermal conductivity (W/m·K)	2022.4	387.6

The LIB module enclosure has inlet and outlet ports for the cooling medium, as shown in Figure 2. An inlet port is on one side at the top of the wall, and the outlet port is on the diagonally opposite side, positioned at bottom of the wall. The design of the inlet

and outlet ports allows for the cooling medium to flow through the LIB module and to fully immerse the LIB module surfaces. This approach can ensure uniform temperature distribution across the LIB module, which helps maintain the optimal working temperature range between 293 and 313 K.

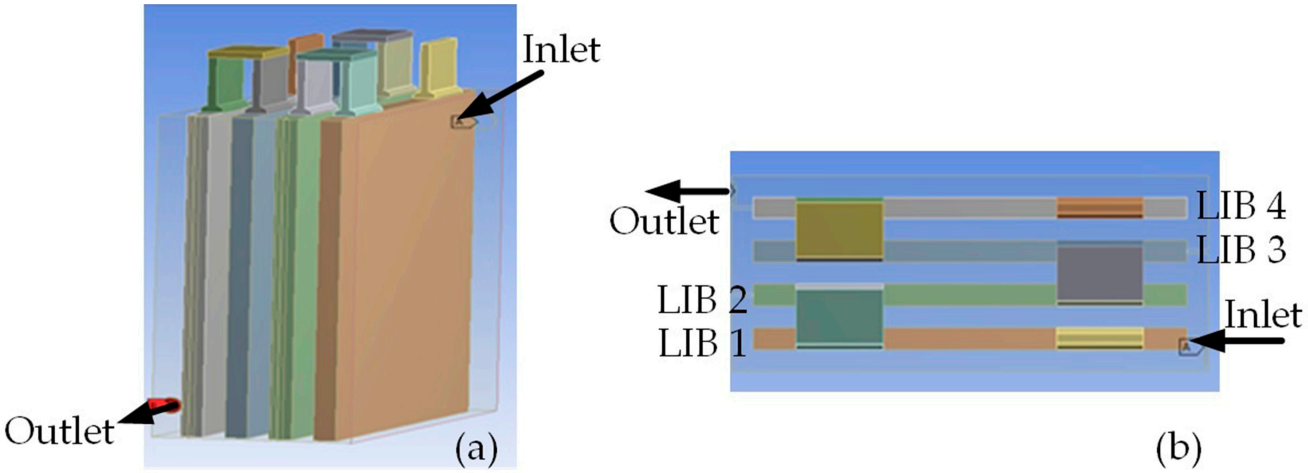

Figure 2. LIB module enclosure design for cooling medium inlet and outlet, in (**a**) isometric view and (**b**) top view.

2.2. Meshing

CFD simulation requires high-quality mesh and appropriate convergence criteria to produce accurate and reliable results without requiring high computational time and power. Hence, mesh convergence is performed to ensure the highest possible accuracy. Two different types of mesh are used for the LIB module enclosure and the LIB module, tetrahedral and structured.

The LIB module enclosure is meshed using tetrahedral elements due to its complex geometry and to avoid any distortion. For the LIB module, hexahedral elements are used with four different element size refinements. Four simulation iterations are run based on the full depletion of the LIB module. The element sizes are set between 2 and 4 mm, with 0.5 mm intervals. The average LIB module maximum temperature is plotted against the number of elements.

As shown in Figure 3, at an element size of 3 mm, the mesh gave a converged model. The differences between the average LIB module maximum temperatures of element sizes 2 mm, 2.5 mm, and 3 mm are negligible. Element sizes of 2 mm and 2.5 mm will require high computational time, but contribute insignificantly to accuracy. Hence, it is more practical to rely on the 3 mm element size. The total number of elements used for the LIB module is 125,068. Figure 4 shows the final mesh for the BTMS (LIB module, enclosure, and coolant medium).

2.3. Input Parameters

In this analysis, the dielectric fuel components (molecules) are utilised as the BTMS coolant. Only fuel components of a dielectric constant $\kappa < 2$ are considered in this model, avoiding any possible short circuit inside the LIB module. To validate the effectiveness of using fuel components as BTMS coolant, they are compared with the conventional coolant (3M Novec-7000).

The 3M Novec-7000 is a dielectric fluid, used for direct liquid cooling in HEV applications or electronic components, as discussed in the literature [22]. It has proven its efficiency in keeping LIBs within the optimal working temperature range at various discharge rates, and maintaining a uniform temperature distribution across the LIBs.

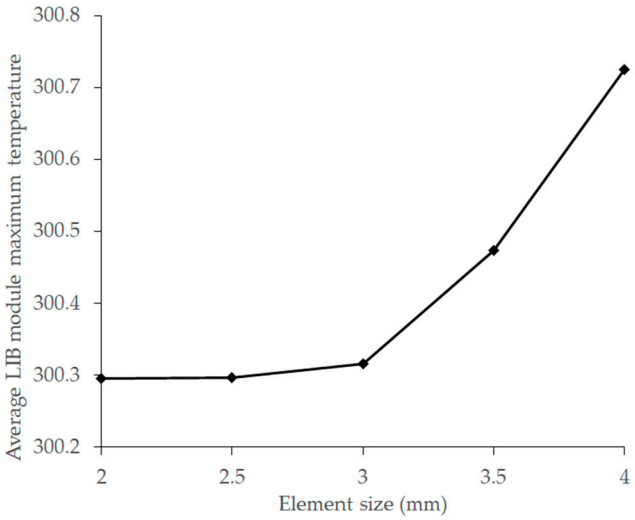

Figure 3. LIB module maximum temperature versus element size, showing the mesh independence check.

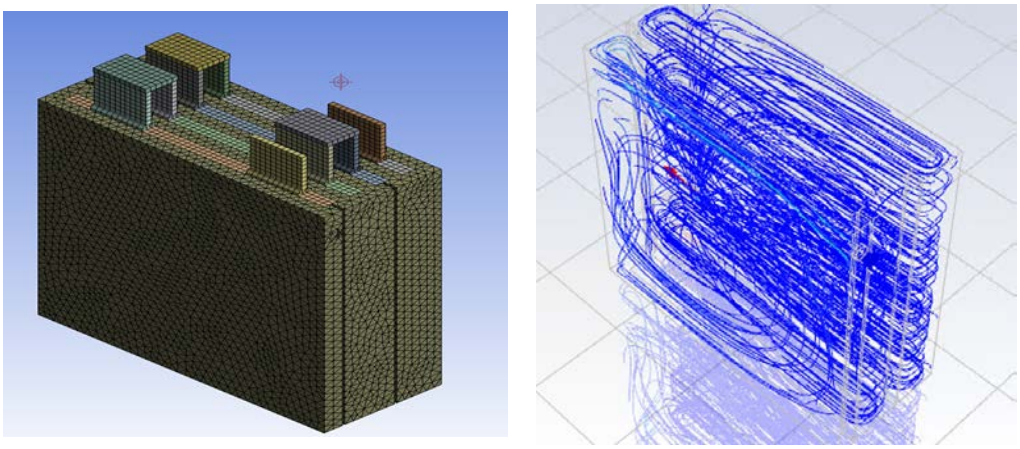

(**a**) (**b**)

Figure 4. LIB module and LIB module enclosure of (**a**) complete mesh and (**b**) flow field of cooling medium.

The cooling medium is set with inlet port temperature of 298 K and outlet port pressure of 1 atmospheric. The flow is simulated for three different inlet velocities: 0.1 m/s, 0.5 m/s, and 1 m/s, to understand the velocity influence on the thermal performance of the LIB module. Additionally, for each of the inlet velocities, three discharge rates are accounted for, 1C, 1.5C, and 2C. The transient discharge effects are considered in a quasi-steady format, with 30-time iterations until the LIB module is fully depleted. The free convection effect is included with the heat transfer coefficient set to 5 $W/m^2 \cdot K$. The turbulence model (K-epsilon) is used for the CFD model, where the cooling medium inside the enclosure is expected to show some turbulent flow.

The properties of the proposed coolants are shown in Table 3. All fuel components have $\kappa < 2$ and reasonably good thermal conductivities, compared to the 3M Novec-7000. These fuel components will be further investigated for their suitability using ANSYS-fluent. In [35], the thermo-physical properties of different fuel components are provided with detailed methods of calculation, embedded in our model.

Table 3. Comparison of thermo-physical properties of fuel components, and 3M Novec-7000 [34,36].

Cooling Medium	Density (kg·m^3)	Constant Specific Heat (J/kg·K)	Thermal Conductivity (W/m·K)	Viscosity (kg/m·s)	κ
N-Pentane	622	2330	0.105	0.0002140	1.84
N-Hexane	653	2260	0.114	0.0002970	1.88
N-Butane	581	1675	0.095	0.0000074	1.77
Cyclo-Pentane	763	1757	0.170	0.0004622	1.97
3M Novec-7000	1400	1300	0.075	0.0004500	7.40

3. Results

The results are based on the main indicators for improving the BTMSs, in terms of temperature value and uniformity. The discharge rates, velocity and types of coolants are the controlling parameters in this study. In what follows, four types of petrol fuels are assessed for use as coolants and compared to the conventional coolants of 3M Novec-7000 and air (inferred from [37]).

3.1. N-Pentane

The temperature behaviour of the LIB module using N-Pentane as a coolant is shown in Table 4. When the inlet velocity is set to 0.1 m/s, the maximum LIB module temperature is maintained within the optimal operating range for all discharge rates, 1C (301.51 K), 1.5C (304.545 K), and 2C (306.534 K). In comparison with the free air convection (FAC)-BTMS results [33], it reduces the maximum temperature of the LIB module at 1C, 1.5C, and 2C by 2.6% (8.10 K), 2.2% (6.92 K), and 3.5% (10.99 K), respectively. When the inlet velocity of N-Pentane is increased to 0.5 m/s, the maximum LIB module temperatures are reduced by 2.5% (9.14 K), 4% (12.50 K), and 5.2% (16.37 K) for 1C, 1.5C, and 2C, respectively. At a higher inlet velocity (1 m/s), the maximum LIB module temperatures at 1C, 1.5C, and 2C are further reduced by 3.3% (10.12 K), 3.4% (10.63 K), and 5.9% (18.74 K), respectively. Since the temperature reduction between 0.5 m/s and 1 m/s is significant, passive control strategies can be implemented for such energy management by regulating the pump speed at high ambient temperatures.

Table 4. Temperature behaviour of the LIB module with N-Pentane LC-BTMS.

LIB Type	1C		1.5C		2C	
	T_{max} (K)	T_{min} (K)	T_{max} (K)	T_{min} (K)	T_{max} (K)	T_{min} (K)
	Cooling medium velocity = 0.1 m/s					
Module	301.516	299.753	304.545	301.437	306.534	302.154
LIB 1	300.729	299.753	303.243	301.437	304.292	302.154
LIB 2	300.81	300.014	303.39	301.813	304.545	302.899
LIB 3	301.263	300.636	304.132	302.907	305.723	304.553
LIB 4	301.516	301.008	304.545	303.557	306.534	305.605
	Cooling medium velocity = 0.5 m/s					
Module	300.478	298.83	300.981	298.963	302.346	299.378
LIB 1	300.149	298.83	300.529	298.963	301.59	299.378
LIB 2	300.178	299.134	300.558	299.348	301.66	299.942
LIB 3	300.305	299.771	300.742	300.33	301.956	301.413
LIB 4	300.478	299.974	300.981	300.627	302.346	301.862
	Cooling medium velocity = 1 m/s					
Module	299.497	298.335	300.834	298.648	301.551	298.788
LIB 1	299.306	298.335	300.472	298.648	301.023	298.788
LIB 2	299.336	298.455	300.545	298.873	301.107	299.073
LIB 3	299.398	299.107	300.659	300.111	301.302	300.572
LIB 4	299.497	299.21	300.834	300.296	301.551	300.818

The constant behaviours of the maximum LIB module temperature at all discharge rates are significantly improved compared to the inlet velocity of 0.1 m/s, which indicates

that the inlet velocity is governed by the heat transfer process between the LIB module and to N-Pentane cooling medium, as shown in Figure 5. One can see that using N-Pentane as a BTMS liquid coolant (LC-BTMS) successfully maintains the LIB module temperature at a constant level within 80% of the total discharge time. This constant temperature behaviour can help to maintain the state of health of LIBs in the long run [10].

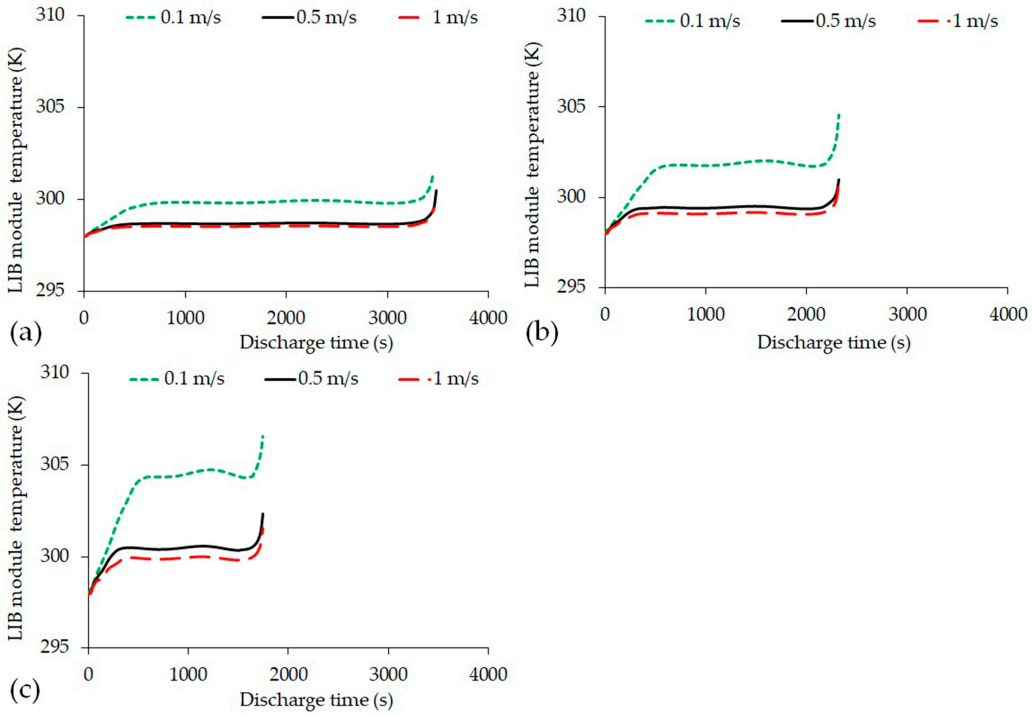

Figure 5. LIB module temperature with N-Pentane LC-BTMS at three inlet velocities (**a**) 1C, (**b**) 1.5C, and (**c**) 2C.

Figure 6 shows the temperature distribution of the LIB module and each of the LIBs. Even though the maximum LIB module temperature is below the maximum threshold value for all discharge rates and inlet velocities, at 2C and an inlet velocity of 0.1 m/s, the surface temperature difference of the LIB module is 146.3% (4.38 K) higher compared to FAC-BTMS. In terms of the maximum LIB temperature difference, N-Pentane also produces lower temperature differences (i.e., maintained homogenous thermal distribution) compared to FAC-BTMS at all discharge rates and inlet velocities. Between LIB 4 and LIB 1, the highest temperature difference is 2.24 K at the highest discharge rate (2C) and at an inlet velocity 1 m/s.

3.2. N-Hexane

At an inlet velocity of 0.1 m/s, N-Hexane LC-BTMS reduces the temperature of the maximum LIB module at 1C, 1.5C, and 2C by 2.7% (8.219 K), 2.3% (7.195 K), and 3.5% (11.262 K), respectively, compared to FAC-BTMS. From Table 5, the inlet velocity of 0.1 m/s is able to maintain the maximum LIB module temperature below 313 K for all discharge rates.

As can be seen from Table 5, the use of N-Hexane as LC-BTMS was useful in reducing the maximum LIB module temperature. For instance, at 0.5 m/s inlet velocity, the LIB module temperature is decreased by 3% at 1C, 4% at 1.5C, and 5.2% at 2C, compared to FAC-BTMS. As the inlet velocity is doubled to 1 m/s, further reductions in the maximum LIB module temperature are received as 3.1%, 3.5%, and 5.9%, lower than the case of FAC-BTMS, obtained at 1C, 1.5C, and 2C, respectively. As can see from the results, the temperature reductions for both 0.5 m/s and 1 m/s are similar. Therefore, to maintain low

pumping power, the inlet velocity of 0.5 m/s can be sufficient to maintain the LIB module temperature within the safe range.

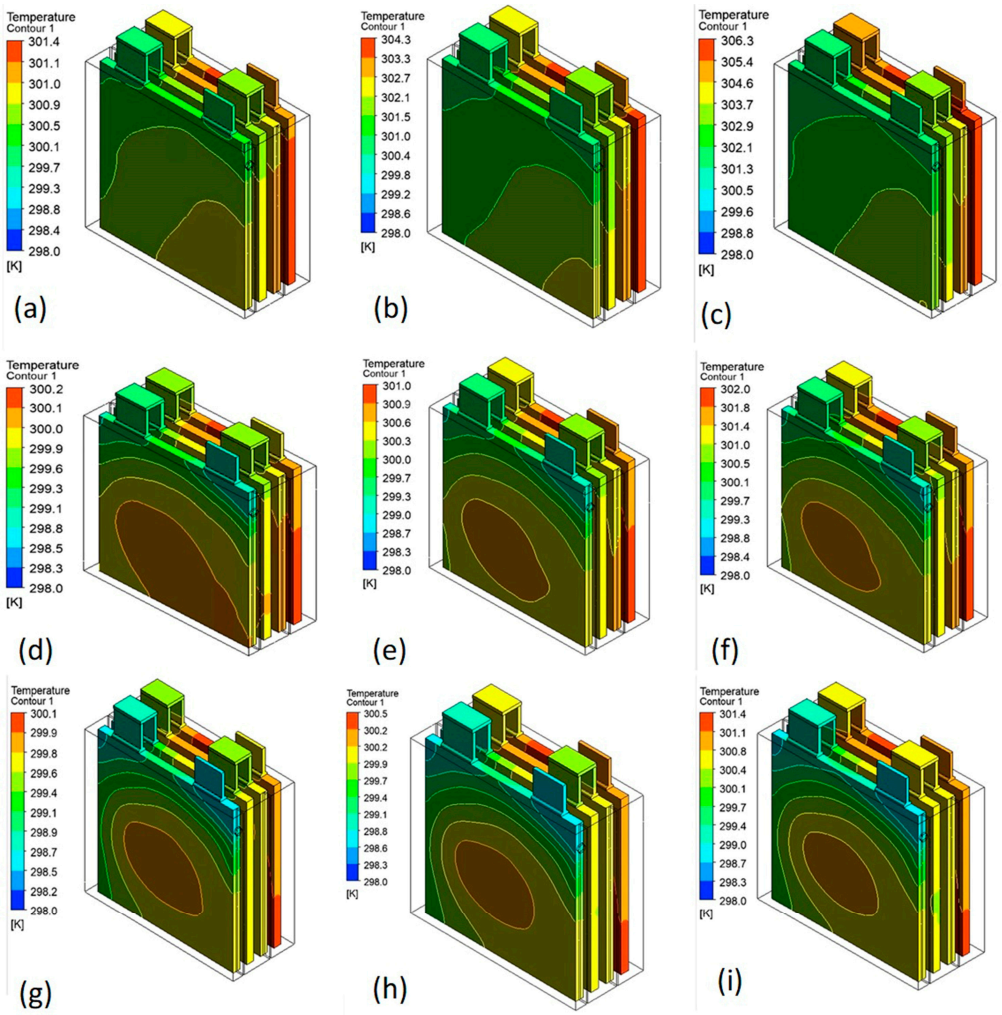

Figure 6. LIB module temperature distribution with N-Pentane LC-BTMS at (**a**) 1C at 0.1 m/s, (**b**) 1.5C at 0.1 m/s, (**c**) 2C at 0.1 m/s, (**d**) 1.5C at 0.5 m/s, (**e**) 1.5C at 0.5 m/s, (**f**) 2C at 0.5 m/s, (**g**) 1C at 1 m/s, (**h**) 1.5C at 1 m/s, and (**i**) 2C at 1 m/s.

Table 5. Temperature behaviour of the LIB module with N-Hexane LC-BTMS.

LIB Type	1C		1.5C		2C	
	T_{max} (K)	T_{min} (K)	T_{max} (K)	T_{min} (K)	T_{max} (K)	T_{min} (K)
Cooling velocity = 0.1 m/s						
Module	301.395	299.630	304.269	301.169	306.264	301.848
LIB 1	300.636	299.630	302.992	301.169	304.058	301.848
LIB 2	300.716	299.937	303.143	301.632	304.312	302.709
LIB 3	301.154	300.570	303.869	302.752	305.453	304.391
LIB 4	301.395	300.921	304.269	303.369	306.264	305.388
Cooling velocity = 0.5 m/s						
Module	300.167	298.762	300.88	298.993	301.932	299.320
LIB 1	299.789	298.762	300.342	298.993	301.077	299.320
LIB 2	299.837	299.067	300.408	299.415	301.17	299.902
LIB 3	300.003	299.567	300.641	300.224	301.534	301.104
LIB 4	300.167	299.764	300.88	300.522	301.932	301.518

Table 5. *Cont.*

LIB Type	1C		1.5C		2C	
	T_{max} (K)	T_{min} (K)	T_{max} (K)	T_{min} (K)	T_{max} (K)	T_{min} (K)
	Cooling velocity = 1 m/s					
Module	299.930	298.494	300.461	298.61	301.399	298.817
LIB 1	299.713	298.494	300.153	298.61	300.871	298.817
LIB 2	299.708	298.676	300.137	298.849	300.863	299.149
LIB 3	299.817	299.45	300.293	299.905	301.154	300.573
LIB 4	299.93	299.576	300.461	300.049	301.399	300.790

The LIB module temperatures at three inlet velocities versus discharge time are presented in Figure 7, based on the three discharge rates, (a) 1C, (b) 1.5C, and (c) 2C. As can be seen from the figure, the results show similar trends to those shown for N-Pentane LC-BTMS. The constant temperature behaviour occurs during the first 80% of the full discharge time.

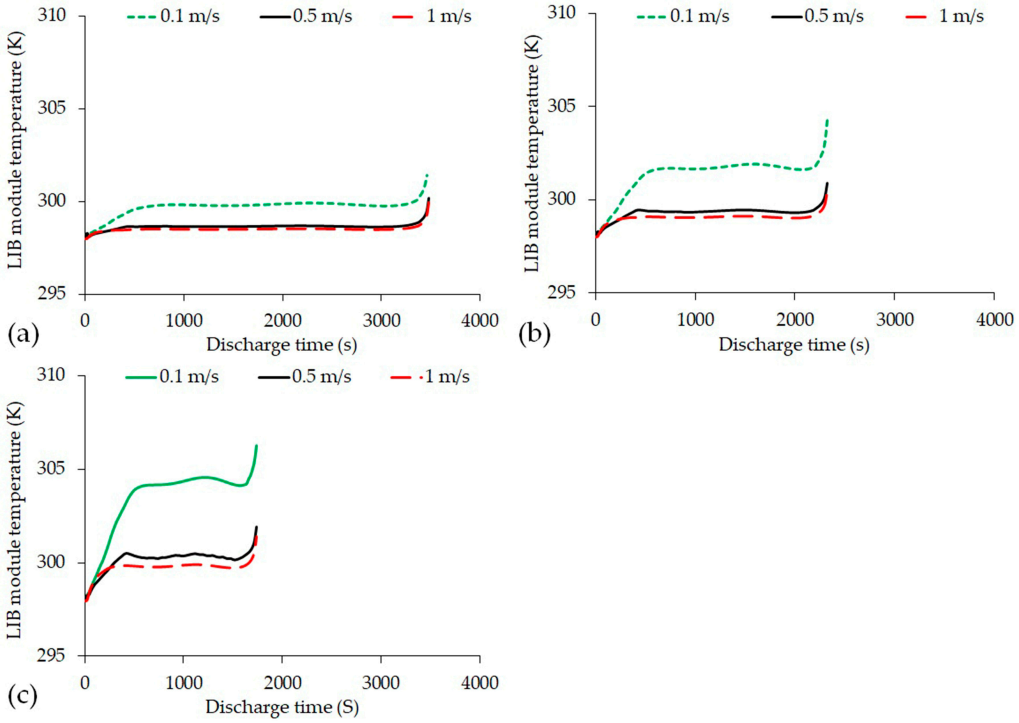

Figure 7. LIB module temperature with N-Hexane liquid-cooled BTMS at three inlet velocities (**a**) 1C, (**b**) 1.5C, and (**c**) 2C.

The temperature contours of the LIB module are illustrated in Figure 8, showing all nine cases of discharge rates and inlet velocities, (a) 1C at 0.1 m/s, (b) 1.5C at 0.1 m/s, (c) 2C at 0.1 m/s, (d) 1.5C at 0.5 m/s, (e) 1.5C at 0.5 m/s, (f) 2C at 0.5 m/s, (g) 1C at 1 m/s, (h) 1.5C at 1 m/s, and (i) 2C at 1 m/s. For instance, at 0.1 m/s and 2C, the LIB module temperature is more homogenous than that of FAC-BTMS, with a 148.4% (4.416 K) less temperature difference. Although using N-Pentane as a coolant showed promising results, using N-Hexane as a coolant further reduced the temperature difference by almost 2.2 °C.

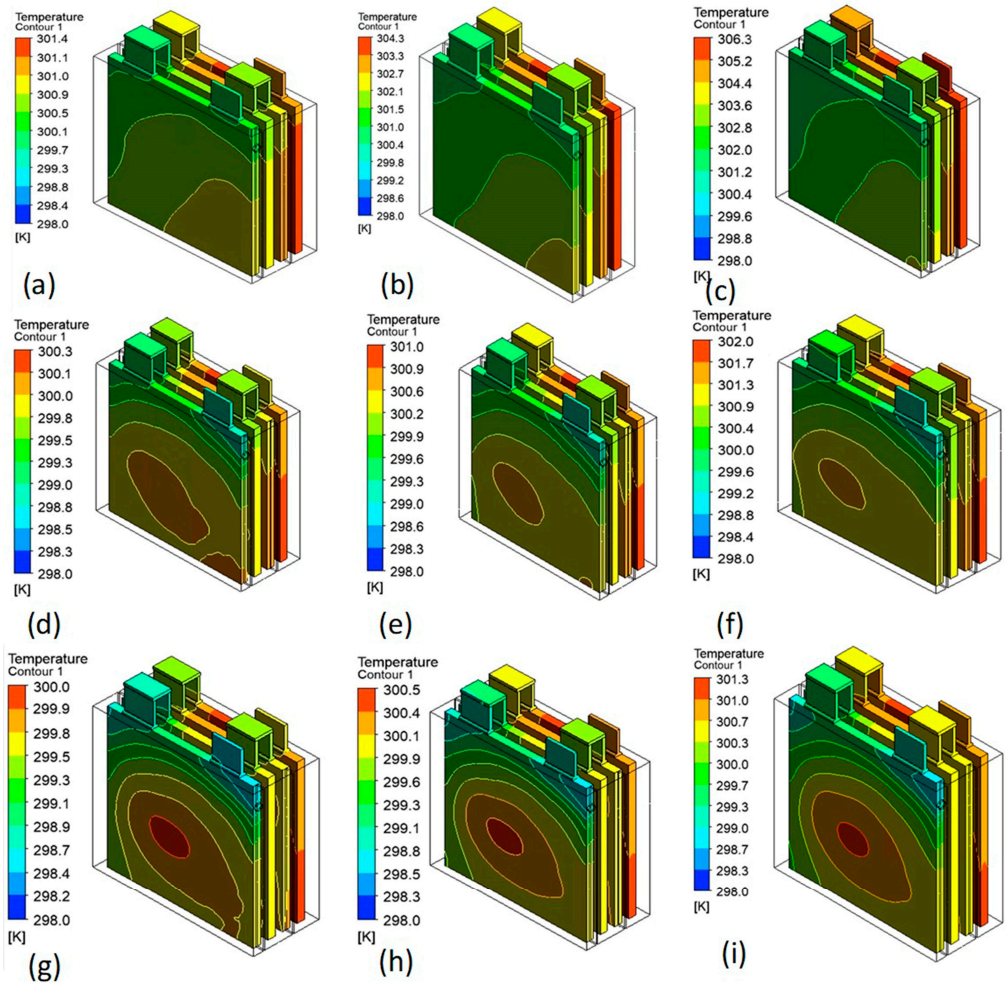

Figure 8. LIB module temperature distribution with N-Hexane LC-BTMS at (**a**) 1C at 0.1 m/s, (**b**) 1.5C at 0.1 m/s, (**c**) 2C at 0.1 m/s, (**d**) 1.5C at 0.5 m/s, (**e**) 1.5C at 0.5 m/s, (**f**) 2C at 0.5 m/s, (**g**) 1C at 1 m/s, (**h**) 1.5C at 1 m/s, and (**i**) 2C at 1 m/s.

3.3. N-Butane

The BTMS using N-Butane is investigated and presented in Table 6. As can be seen from Table 6, using N-Butane as a coolant in BTMS, the temperature values and distribution are reasonably good. At an inlet velocity of 0.1 m/s, N-Butane LC-BTMS has a slightly better cooling performance than N-Heptane LC-BTMS at higher discharge rates. In comparison to FAC-BTMS, N-Butane decreases the maximum LIB module temperature by 2.0% (6.16 K), 2.5% (7.85 K), and 3.6% (11.57 K) at 1C, 1.5C, and 2C, respectively. When the inlet velocity of the cooling medium is increased to 0.5 m/s, the maximum LIB temperatures are decreased to 300.075K (at 1C), 302.217 K (at 1.5C), and 303.032 K (at 2C), which reduce the maximum temperature by 3.8% below the maximum threshold temperature (307 K). At 1 m/s, the maximum LIB module temperatures at 1C, 1.5C, and 2C are further reduced by 3.1% (9.60 K), 3.4% (10.88 K), and 5.9% (18.65 K), respectively. The temperature trends at both inlet velocities, 0.5 m/s and 1 m/s, are similar, especially at 1C and 1.5C; i.e., the pump speed can be reduced to maintain the same system efficiency. The temperatures versus discharge time for N-Butane are presented in Figure 9, which shows similar trends to those seen for other fuels. Nevertheless, the maximum LIB module temperatures tend to plateau for the first 80% of the full discharge time.

Table 6. Temperature behaviour of the LIB module with N-Butane LC-BTMS.

LIB Type	1C		1.5C		2C	
	T_{max} (K)	T_{min} (K)	T_{max} (K)	T_{min} (K)	T_{max} (K)	T_{min} (K)
Cooling velocity = 0.1 m/s						
Module	303.456	300.15	303.611	300.975	305.957	301.957
LIB 1	301.647	300.15	302.211	300.975	303.522	301.957
LIB 2	302.19	300.586	302.349	301.355	303.731	302.626
LIB 3	302.914	301.926	303.104	302.164	304.857	303.854
LIB 4	303.456	302.396	303.611	302.823	305.753	304.879
Cooling velocity = 0.5 m/s						
Module	300.075	298.474	302.217	299.042	303.032	299.112
LIB 1	299.338	298.474	300.924	299.042	301.202	299.112
LIB 2	299.685	298.545	301.507	299.190	301.923	299.283
LIB 3	299.901	299.275	301.923	300.742	302.574	301.023
LIB 4	300.075	299.607	302.217	301.348	303.032	301.830
Cooling velocity = 1 m/s						
Module	300.013	298.383	300.631	298.483	302.575	298.877
LIB 1	299.372	298.393	299.703	298.483	301.118	298.877
LIB 2	299.711	298.456	300.212	298.562	301.841	299.02
LIB 3	299.901	299.148	300.457	299.409	302.309	300.592
LIB 4	300.013	299.464	300.631	299.826	302.575	301.316

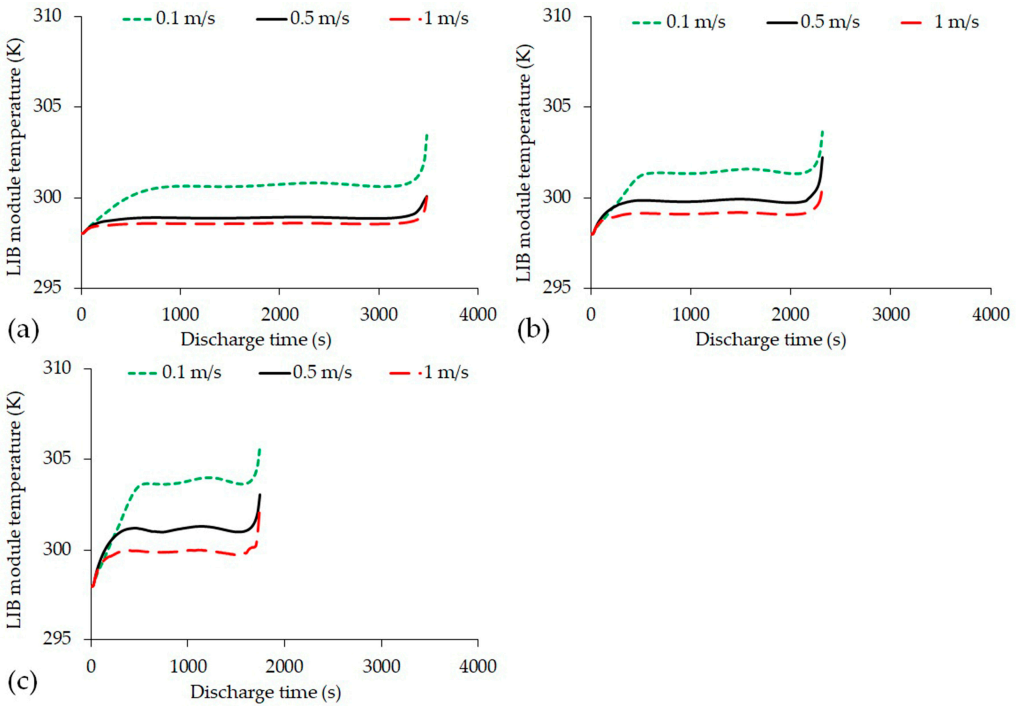

Figure 9. LIB module temperature with N-Butane LC-BTMS at three inlet velocities (**a**) 1C, (**b**) 1.5C, and (**c**) 2C.

In terms of the temperature distribution of the LIB module and the comparison with FAC-BTMS, the maximum temperature difference still occurs at 2C and an inlet velocity of 0.1 m/s (higher by 125% or 4.00 K). This temperature difference, however, is slightly better than N-Heptane and N-Pentane LC-BTMS. The LIB module temperature distributions are shown in Figure 10.

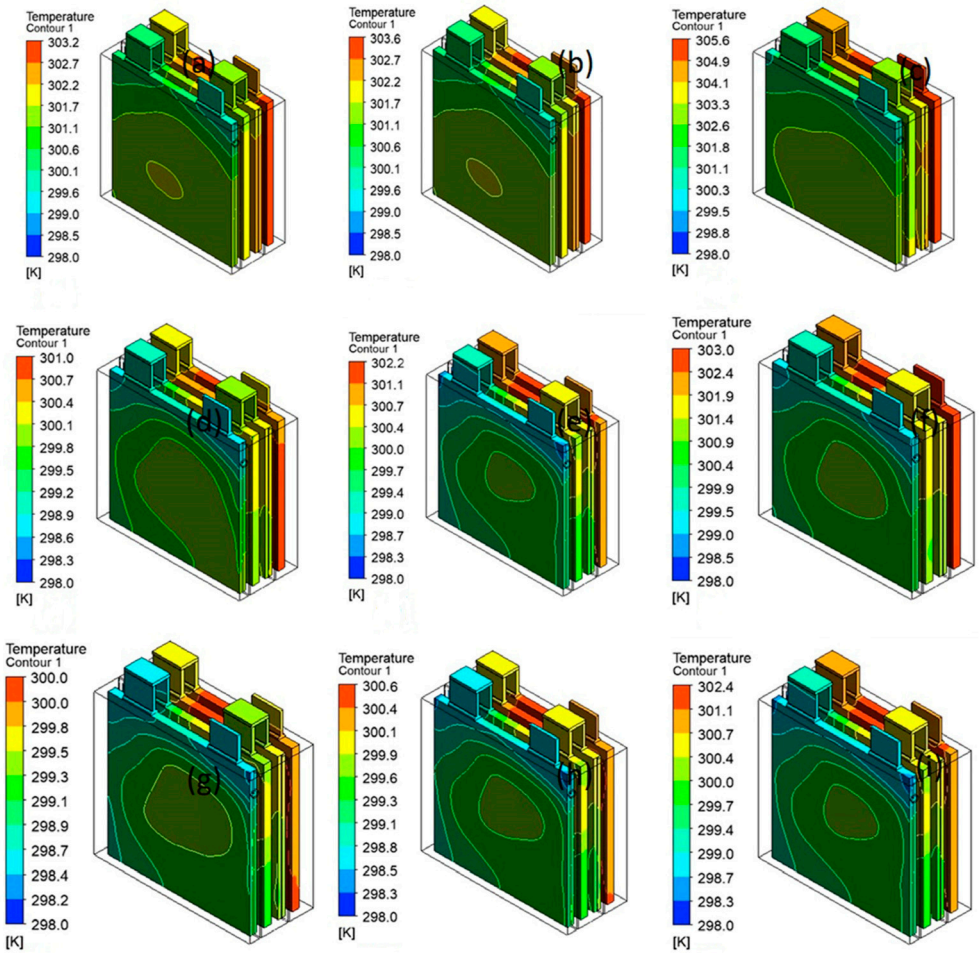

Figure 10. LIB module temperature distribution with N-Butane LC-BTMS at (**a**) 1C at 0.1 m/s, (**b**) 1.5C at 0.1 m/s, (**c**) 2C at 0.1 m/s, (**d**) 1.5C at 0.5 m/s, (**e**) 1.5C at 0.5 m/s, (**f**) 2C at 0.5 m/s, (**g**) 1C at 1 m/s, (**h**) 1.5C at 1 m/s, and (**i**) 2C at 1 m/s.

In terms of the LIB temperature difference, N-Butane LC-BTMS produces the highest temperature difference of 2.922 K between LIB 4 and LIB 1. This temperature behaviour occurs at an inlet velocity of 0.1 m/s and a discharge rate of 1C, at a different parameter setting from those of N-Hexane and N-Pentane LC-BTMS.

3.4. Cyclo-Pentane

Compared to FAC-BTMS, Cyclo-Pentane LC-BTMS manages to reduce the maximum LIB module temperature by 2.6% (8.08 K), 2.3% (7.23 K), and 3.4% (10.85 K) at an inlet velocity of 0.1 m/s and 1C, 1.5C, and 2C, respectively. As shown in Table 7, the inlet velocity of 0.1 m/s is able to maintain the maximum LIB module temperature below 313 K for all discharge rates. When the inlet velocity of the cooling medium is increased to 0.5 m/s, the maximum LIB temperatures are reduced to 300.422 K (1C), 300.999 K (1.5C), and 301.822 K (2C), which provides the same average as N-Butane LC-BTMS, 3.8% below the maximum threshold temperature.

Table 7. Temperature behaviour of the LIB module with Cyclo-Pentane LC-BTMS.

LIB Type	1C		1.5C		2C	
	T_{max} (K)	T_{min} (K)	T_{max} (K)	T_{min} (K)	T_{max} (K)	T_{min} (K)
Cooling velocity = 0.1 m/s						
Module	301.539	299.525	304.236	300.736	306.674	301.561
LIB 1	300.8	299.525	302.947	300.736	304.537	301.561
LIB 2	300.898	299.934	303.131	301.464	304.841	302.783
LIB 3	301.33	300.670	303.870	302.784	306.005	304.783
LIB 4	301.539	300.986	304.236	303.345	306.674	305.699
Cooling velocity = 0.5 m/s						
Module	300.422	298.816	300.999	298.983	301.822	299.243
LIB 1	299.825	298.816	300.188	298.983	300.736	299.2243
LIB 2	299.920	299.178	300.323	299.452	300.922	299.860
LIB 3	300.187	299.591	300.681	300.127	301.399	300.856
LIB 4	300.422	299.841	300.999	300.489	301.822	301.36
Cooling velocity = 1 m/s						
Module	299.736	298.444	299.879	298.462	300.665	298.644
LIB 1	299.498	298.444	299.585	298.462	300.189	298.644
LIB 2	299.474	298.637	299.548	298.68	300.144	298.951
LIB 3	299.592	299.262	299.701	299.441	300.432	299.999
LIB 4	299.736	299.416	299.879	299.604	300.665	300.234

By doubling the inlet velocity of the cooling medium to 1 m/s, the maximum LIB module temperatures are further reduced to 299.74 K, 299.88 K, and 300.67 K at 1C, 1.5C, and 2C, respectively. These temperature reductions are not significant compared to the temperature at the inlet velocity of 0.5 m/s. Hence, it is recommended not to adopt a higher inlet velocity of more than 0.5 m/s for energy management strategy benefits. As shown in Figure 11, the maximum LIB module temperatures have a steady trend (more than 80% of the discharge time) for Cyclo-Pentane liquid-cooled at all discharge rates, which are similar to other fuel components.

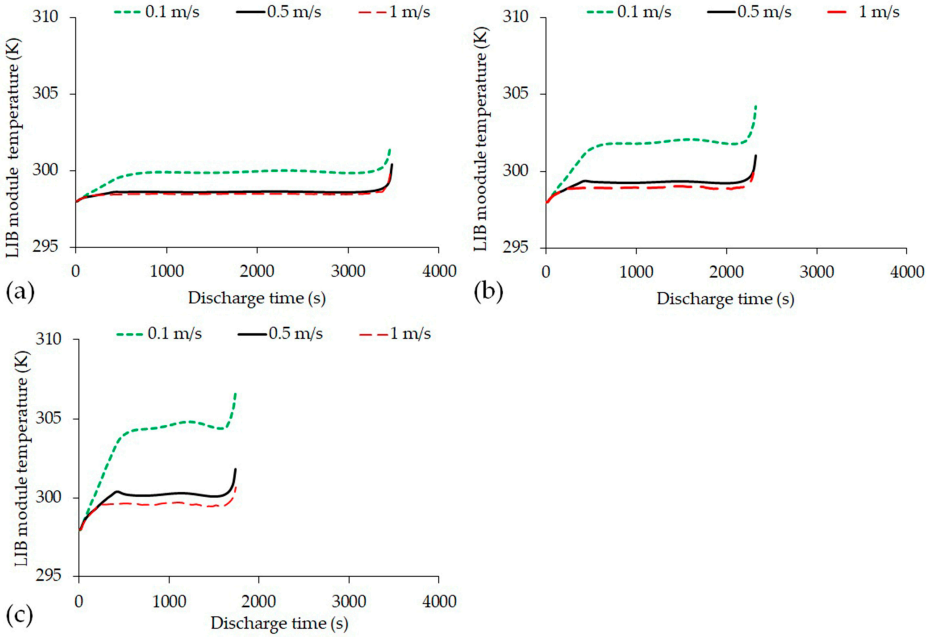

Figure 11. LIB module temperature with Cyclo-Pentane liquid-cooled BTMS at three inlet velocities (**a**) 1C, (**b**) 1.5C, and (**c**) 2C.

The maximum temperature distribution of Cyclo-Pentane LC-BTMS is significantly poorer than that of other fuel components, with the highest temperature difference of 5.11 K

at 0.1 m/s of inlet velocity and 2C. From Figure 12, the LIB cell temperature difference is also the highest compared to the other fuel components for LIB 4 and LIB 1, with a temperature difference of 4.138 K at an inlet velocity of 0.1 m/s and 2C.

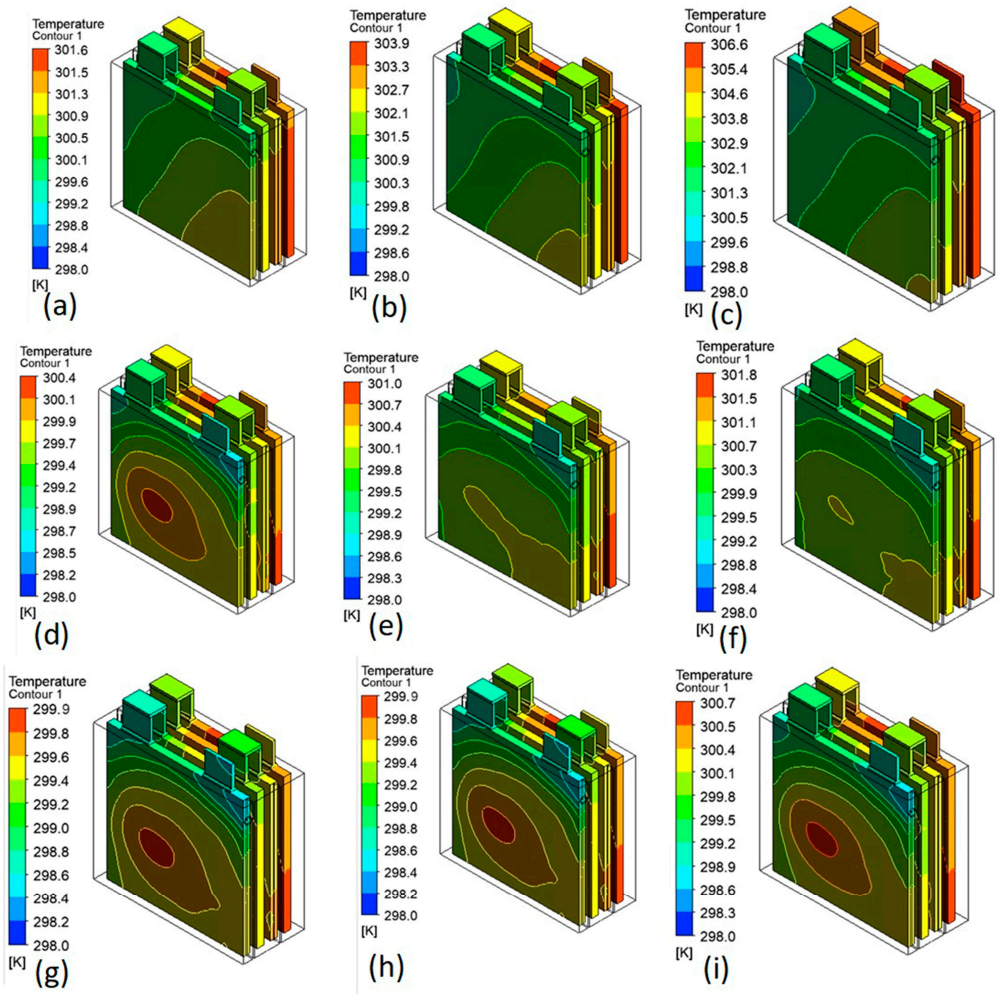

Figure 12. LIB module temperature distribution with Cyclo-Pentane LC-BTMS at (**a**) 1C at 0.1 m/s, (**b**) 1.5C at 0.1 m/s, (**c**) 2C at 0.1 m/s, (**d**) 1.5C at 0.5 m/s, (**e**) 1.5C at 0.5 m/s, (**f**) 2C at 0.5 m/s, (**g**) 1C at 1 m/s, (**h**) 1.5C at 1 m/s, and (**i**) 2C at 1 m/s.

3.5. Comparative Analysis

A comparative analysis is conducted to validate the performance of fuel components LC-BTMS against 3M Novec-7000 (conventional cooling medium) in the worst-case scenario at 2C and an inlet velocity of 0.5 m/s. As can be seen in Figure 13, all of the fuel components in the LC-BTMS system, with the exception of N-Butane LC-BTMS, have better cooling performance than the 3M Novec-7000 LC-BTMS. The results of this study suggest that the fuel component LC-BTMS has the potential as a cooling medium to maintain the temperature of LIB and can reduce the design complexity of BTMS. It is possible that integrating the fueling system and BTMS could help reduce vehicle weight and improve overall energy consumption.

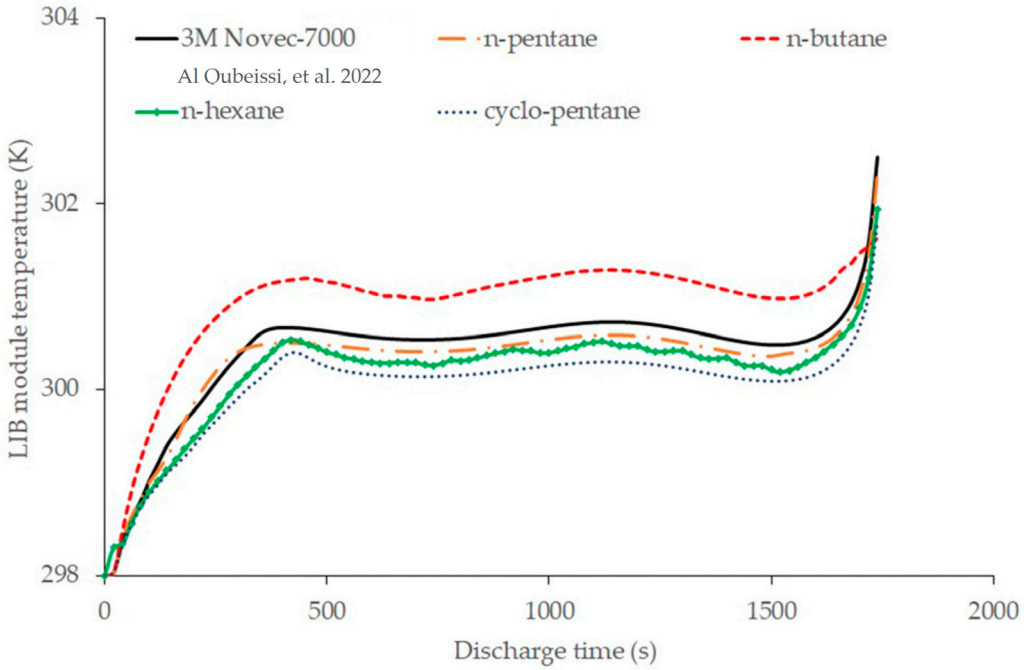

Figure 13. Comparative analysis of LC-BTMS, fuel components vs. 3M Novec-7000 [33] at 2C and an inlet velocity of 0.5 m/s.

To verify the accuracy of the CFD model, FAC-BTMS is compared with the previous work performed by [33]. Table 8 shows the LIB temperature behaviour of the module and cells at three discharge rates. As shown in Figure 14, 1C, 1.5C, and 2C require 3480 s, 2340 s, and 1740 s, respectively, to fully deplete the LIB module.

Table 8. Maximum and minimum temperatures of the LIB module with FAC-BTMS.

LIB Type	1C		1.5C		2C	
	T_{max} (K)	T_{min} (K)	T_{max} (K)	T_{min} (K)	T_{max} (K)	T_{min} (K)
Module	309.614	307.208	311.464	310.261	317.526	315.748
LIB 1	309.614	307.568	311.464	310.428	317.526	316.006
Lib 2	309.587	307.551	311.436	310.422	317.481	315.997
LIB 3	309.587	308.55	311.436	310.422	317.481	315.997
LIB 4	309.614	307.568	311.464	310.428	317.526	316.006

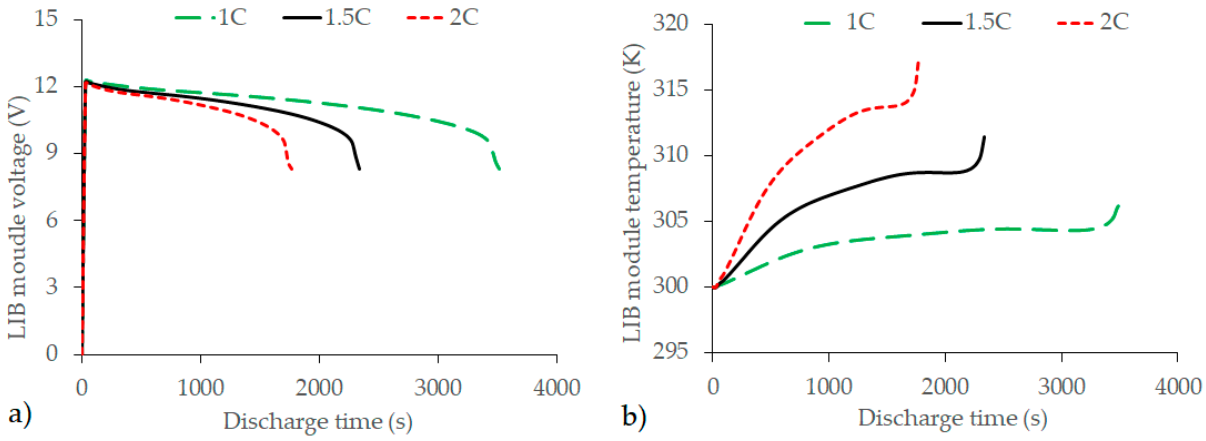

Figure 14. LIB module behaviour at three discharge rates with FAC-BTMS (**a**) LIB module voltage and (**b**) LIB module temperature.

The maximum LIB module temperatures have the same values, 309.614 K, 311.464 K, and 317.526 K at 1C, 1.5C, and 2C, respectively. These results demonstrate that the CFD model is a valuable tool for evaluating the performance of fuel component LC-BTMS and can assist in the development of effective BTMS strategies.

4. Conclusions

LIB module temperature without any cooling at the ambient condition of 298 K and 2C exceeds the maximum threshold temperature and can lead to thermal runaway. Hence, an efficient BTMS is required to maintain the optimal working temperature. Some fuel components, such as N-Pentane, N-Hexane, N-Butane, and Cyclo-Pentane, show the potential for coolants in direct cooling of LIB due to their dielectric constants (< 2). The cooling performance of fuel as LC-BTMS (liquid-coolant in battery thermal management system) in the HEVs application was successfully simulated using commercial CFD modelling, ANSYS-Fluent software. The CFD model shows a good agreement with the literature data and can be extended for different cooling media applications to characterise the thermal management of LIB modules.

The results demonstrate that at all discharge rates, the maximum LIB module temperature is managed at:

- 301.526 K (1C), 304.545 K (1.5), and 306.534 K (2C) for N-Pentane LC-BTMS at inlet velocity 0.1 m/s, indicating an average reduction of 2.8% compared to FAC-BTMS.
- 299.497 K (1C), 300.834 K (1.5C), and 301.551 K(2C) for N-Pentane LC-BTMS at inlet velocity 1 m/s, indicating an average reduction of 3.9% compared to FAC-BTMS.;
- 301.395 K (1C), 304.269 K (1.5), and 306.264 K (2C) for N-Hexane LC-BTMS at inlet velocity 0.1 m/s, indicating an average reduction of 2.8%.
- 299.93 K (1C), 300.461 K (1.5C), and 301.399 K(2C) for N-Hexane LC-BTMS at inlet velocity 1 m/s, indicating an average reduction of 3.9%.
- 303.456 K (1C), 303.611 K (1.5), and 305.957 K (2C) for N-Butane LC-BTMS at inlet velocity 0.1 m/s, indicating an average reduction of 2.7%.
- 300.013 K (1C), 300.631 K (1.5C), and 302.575 K(2C) for N-Butane LC-BTMS at inlet velocity 1 m/s, indicating an average reduction of 3.8%.
- 301.539 K (1C), 3304.236 K (1.5), and 306.674 K (2C) for Cyclo-Pentane LC-BTMS at inlet velocity 0.1 m/s, indicating an average reduction of 2.8%.
- 299.736 K (1C), 299.879 K (1.5C), and 300.665 K(2C) for Cyclo-Pentane LC-BTMS at inlet velocity 1 m/s, with an average reduction of 4.1%.compared to FAC-BTMSs.

Also, it is noted that N-Pentane, N-Hexane, N-Butane, and Cyclo-Pentane produce an average temperature difference of -0.101 K, -0.232 K, 0.490 K, and -0.380 K, respectively, below that of 3M Novec-7000 LC-BTMS. Additionally, all fuel component LC-BTMSs are able to maintain the temperature difference between LIB cells below 5 K.

To conclude, the relatively low density of these fuel components can help in reducing the overall mass of the vehicle and improve its energy consumption which makes these fuel components viable alternatives to conventional cooling media. It is important to note the flammability of fuels when used in BTMSs. As such, indirect cooling can be more feasible in practice, when the temperature range exceeds the advised temperature limited in this research finding.

Author Contributions: Conceptualisation, M.A.Q.; data curation, R.M.R.A.S.; investigation, H.Y.; project administration, M.A.Q. and H.S.S.; resources, M.A.Q. and R.M.R.A.S.; software, M.A.Q. and H.Y.; supervision, M.A.Q. and R.M.R.A.S.; writing—original draft, H.Y., R.M.R.A.S. and M.A.Q.; writing—review and editing, M.A.Q. and R.M.R.A.S. All authors have read and agreed to the published version of the manuscript.

Funding: This research received no external funding.

Institutional Review Board Statement: Not applicable.

Informed Consent Statement: Not applicable.

Data Availability Statement: Data is unavailable due to privacy and link to the continuing study.

Conflicts of Interest: The authors declare no conflict of interest.

References

1. Nickischer, A. Environmental Impacts of Internal Combustion Engines and Electric Battery Vehicles. *DU Quark* **2020**, *4*, 21–31.
2. Xia, G.; Cao, L.; Bi, G. A Review on Battery Thermal Management in Electric Vehicle Application. *J. Power Source* **2017**, *367*, 90–105. [CrossRef]
3. Shah, R.M.R.A.; McGordon, A.; Rahman, M.M.; Amor-Segan, M.; Jennings, P. Characterisation of Micro Turbine Generator as a Range Extender Using an Automotive Drive Cycle for Series Hybrid Electric Vehicle Application. *Appl. Therm. Eng.* **2021**, *184*, 116302. [CrossRef]
4. Sawant, S.; Shah, R.M.R.A.; Rahman, M.; Smith, S.; Jumahat, A. *System Modelling of an Electric Two-Wheeled Vehicle for Energy Management Optimization Study*; Collections; Kyushu University Library: Fukuoka, Japan, 2021.
5. Funke, S.Á.; Sprei, F.; Gnann, T.; Plötz, P. How Much Charging Infrastructure Do Electric Vehicles Need? A Review of the Evidence and International Comparison. *Transp. Res. Part D Transp. Environ.* **2019**, *77*, 224–242. [CrossRef]
6. Shah, R.M.R.A.; Qubeissi, M.A.; McGordon, A.; Amor-Segan, M.; Jennings, P. Micro Gas Turbine Range Extender Performance Analysis Using Varying Intake Temperature. *Automot. Innov.* **2020**, *3*, 356–365. [CrossRef]
7. Ma, S.; Jiang, M.; Tao, P.; Song, C.; Wu, J.; Wang, J.; Deng, T.; Shang, W. Temperature Effect and Thermal Impact in Lithium-Ion Batteries: A Review. *Prog. Nat. Sci. Mater. Int.* **2018**, *28*, 653–666. [CrossRef]
8. Sato, N. Thermal Behavior Analysis of Lithium-Ion Batteries for Electric and Hybrid Vehicles. *J. Power Source* **2001**, *99*, 70–77. [CrossRef]
9. Peng, X.; Cui, X.; Liao, X.; Garg, A. A Thermal Investigation and Optimization of an Air-Cooled Lithium-Ion Battery Pack. *Energies* **2020**, *13*, 2956. [CrossRef]
10. Lyu, Y.; Siddique, A.R.M.; Majid, S.H.; Biglarbegian, M.; Gadsden, S.A.; Mahmud, S. Electric Vehicle Battery Thermal Management System with Thermoelectric Cooling. *Energy Rep.* **2019**, *5*, 822–827. [CrossRef]
11. Liu, H.; Wei, Z.; He, W.; Zhao, J. Thermal Issues about Li-Ion Batteries and Recent Progress in Battery Thermal Management Systems: A Review. *Energy Convers. Manag.* **2017**, *150*, 304–330. [CrossRef]
12. Kim, T.; Song, W.; Son, D.-Y.; Ono, L.K.; Qi, Y. Lithium-Ion Batteries: Outlook on Present, Future, and Hybridized Technologies. *J. Mater. Chem. A* **2019**, *7*, 2942–2964. [CrossRef]
13. Bai, Y.; Li, L.; Li, Y.; Chen, G.; Zhao, H.; Wang, Z.; Wu, C.; Ma, H.; Wang, X.; Cui, H.; et al. Reversible and Irreversible Heat Generation of NCA/Si–C Pouch Cell during Electrochemical Energy-Storage Process. *J. Energy Chem.* **2019**, *29*, 95–102. [CrossRef]
14. On-Line Scheme for Parameter Estimation of Nonlinear Lithium Ion Battery Equivalent Circuit Models Using the Simplified Refined Instrumental Variable Method for a Modified Wiener Continuous-Time Model—ScienceDirect. Available online: https://www.sciencedirect.com/science/article/pii/S0306261917308991?via%3Dihub (accessed on 25 October 2022).
15. Review—Reversible Heat Effects in Cells Relevant for Lithium-Ion Batteries—IOPscience. Available online: https://iopscience.iop.org/article/10.1149/1945-7111/abfd73 (accessed on 25 October 2022).
16. Wang, Q.; Ping, P.; Zhao, X.; Chu, G.; Sun, J.; Chen, C. Thermal Runaway Caused Fire and Explosion of Lithium Ion Battery. *J. Power Source* **2012**, *208*, 210–224. [CrossRef]
17. An, Z.; Jia, L.; Ding, Y.; Dang, C.; Li, X. A Review on Lithium-Ion Power Battery Thermal Management Technologies and Thermal Safety. *J. Therm. Sci.* **2017**, *26*, 391–412. [CrossRef]
18. Luo, J.; Zou, D.; Wang, Y.; Wang, S.; Huang, L. Battery Thermal Management Systems (BTMs) Based on Phase Change Material (PCM): A Comprehensive Review. *Chem. Eng. J.* **2022**, *430*, 132741. [CrossRef]
19. Lin, J.; Liu, X.; Li, S.; Zhang, C.; Yang, S. A Review on Recent Progress, Challenges and Perspective of Battery Thermal Management System. *Int. J. Heat Mass Transf.* **2021**, *167*, 120834. [CrossRef]
20. Zhao, C.; Zhang, B.; Zheng, Y.; Huang, S.; Yan, T.; Liu, X. Hybrid Battery Thermal Management System in Electrical Vehicles: A Review. *Energies* **2020**, *13*, 6257. [CrossRef]
21. Tan, X.; Lyu, P.; Fan, Y.; Rao, J.; Ouyang, K. Numerical Investigation of the Direct Liquid Cooling of a Fast-Charging Lithium-Ion Battery Pack in Hydrofluoroether. *Appl. Therm. Eng.* **2021**, *196*, 117279. [CrossRef]
22. Thakur, A.K.; Prabakaran, R.; Elkadeem, M.R.; Sharshir, S.W.; Arıcı, M.; Wang, C.; Zhao, W.; Hwang, J.-Y.; Saidur, R. A State of Art Review and Future Viewpoint on Advance Cooling Techniques for Lithium–Ion Battery System of Electric Vehicles. *J. Energy Storage* **2020**, *32*, 101771. [CrossRef]
23. Chen, D.; Jiang, J.; Kim, G.-H.; Yang, C.; Pesaran, A. Comparison of Different Cooling Methods for Lithium Ion Battery Cells. *Appl. Therm. Eng.* **2016**, *94*, 846–854. [CrossRef]
24. Pesaran, A. Battery Thermal Management in EVs and HEVs: Issues and Solutions. *Battery Man* **2001**, *43*, 34–49.
25. Akbarzadeh, M.; Kalogiannis, T.; Jaguemont, J.; Jin, L.; Behi, H.; Karimi, D.; Beheshti, H.; Van Mierlo, J.; Berecibar, M. A Comparative Study between Air Cooling and Liquid Cooling Thermal Management Systems for a High-Energy Lithium-Ion Battery Module. *Appl. Therm. Eng.* **2021**, *198*, 117503. [CrossRef]
26. Kim, J.; Oh, J.; Lee, H. Review on Battery Thermal Management System for Electric Vehicles. *Appl. Therm. Eng.* **2019**, *149*, 192–212. [CrossRef]

27. Noël, J.A.; Kahwaji, S.; Desgrosseilliers, L.; Groulx, D.; White, M.A. 22—Phase Change Materials. In *Storing Energy*, 2nd ed.; Letcher, T.M., Ed.; Elsevier: Amsterdam, The Netherlands, 2022; pp. 503–535. ISBN 978-0-12-824510-1.
28. Wang, Y.; Wang, Z.; Min, H.; Li, H.; Li, Q. Performance Investigation of a Passive Battery Thermal Management System Applied with Phase Change Material. *J. Energy Storage* **2021**, *35*, 102279. [CrossRef]
29. Buidin, T.I.C.; Mariasiu, F. Battery Thermal Management Systems: Current Status and Design Approach of Cooling Technologies. *Energies* **2021**, *14*, 4879. [CrossRef]
30. Mbulu, H.; Laoonual, Y.; Wongwises, S. Experimental Study on the Thermal Performance of a Battery Thermal Management System Using Heat Pipes. *Case Stud. Therm. Eng.* **2021**, *26*, 101029. [CrossRef]
31. Nasir, F.; Abdullah, M.Z.; Ismail, M. Experimental Investigation on the Heat Transfer Performance of Heat Pipes in Cooling Hev Lithium-Ion Batteries. *Heat Transf. Res.* **2018**, *49*, 1745–1760. [CrossRef]
32. Wang, R.; Liang, Z.; Souri, M.; Esfahani, M.N.; Jabbari, M. Numerical Analysis of Lithium-Ion Battery Thermal Management System Using Phase Change Material Assisted by Liquid Cooling Method. *Int. J. Heat Mass Transf.* **2022**, *183*, 122095. [CrossRef]
33. Al Qubeissi, M.; Almshahy, A.; Mahmoud, A.; Al-Asadi, M.T.; Raja Ahsan Shah, R.M. Modelling of Battery Thermal Management: A New Concept of Cooling Using Fuel. *Fuel* **2022**, *310*, 122403. [CrossRef]
34. Dielectric Constant. Available online: https://macro.lsu.edu/howto/solvents/Dielectric%20Constant%20.htm (accessed on 12 July 2022).
35. Al Qubeissi, M.; Sazhin, S.S.; Turner, J.; Begg, S.; Crua, C.; Heikal, M.R. Modelling of Gasoline Fuel Droplets Heating and Evaporation. *Fuel* **2015**, *159*, 373–384. [CrossRef]
36. Liquids and Fluids—Specific Heats. Available online: https://www.engineeringtoolbox.com/specific-heat-fluids-d_151.html (accessed on 12 July 2022).
37. Al Qubeissi, M.; Mahmoud, A.; Al-Damook, M.; Almshahy, A.; Khatir, Z.; Soyhan, H.S.; Raja Ahsan Shah, R.M. Comparative Analysis of Battery Thermal Management System Using Biodiesel Fuels. *Energies* **2023**, *16*, 565. [CrossRef]